

ORIGINAL ARTICLE

Exposure–Response Analysis of Necitumumab Efficacy in Squamous Non-Small Cell Lung Cancer Patients

E Chigutsa¹, AJ Long¹ JE Wallin^{2*}

We sought to describe the exposure–response relationship of necitumumab efficacy in squamous non-small cell lung cancer patients and evaluate intrinsic and extrinsic patient descriptors that may guide dosing. SQUIRE was a phase III study comparing necitumumab in combination with gemcitabine and cisplatin vs. gemcitabine and cisplatin alone in 1,014 patients. An integrated model for tumor size dynamics and overall survival was developed, where reduction in tumor size results in a decrease in survival hazard. The change in tumor size was characterized using linear growth and first-order shrinkage. Overall survival was described using a combination of a Weibull function and Gompertz function for the hazard, with dynamic tumor size being a predictor for the hazard. Although body weight resulted in higher clearance and lower exposure, simulations showed that an 800 mg flat dose provided optimal response regardless of body weight.

CPT Pharmacometrics Syst. Pharmacol. (2017) 6, 560–568; doi:10.1002/psp4.12209; published online 13 July 2017.

Study Highlights

WHAT IS THE CURRENT KNOWLEDGE ON THE TOPIC?

☑ The therapeutic anti-EGFR antibody necitumumab has demonstrated significant antitumor activity in colon, non-small cell lung, pancreatic, and squamous cervical cancer models. The pharmacokinetics of necitumumab has been evaluated in a population pharmacokinetic (PK) analysis across studies. Necitumumab exhibits non-linear PK, indicating target-mediated drug disposition, as commonly observed with monoclonal antibodies. Covariate analysis did not indicate any patient factors such as gender, age, race, disease status, renal, or hepatic function, while weight had a small contribution

WHAT QUESTION DID THIS STUDY ADDRESS?

☑ The objective was to quantify the exposure–response of necitumumab on tumor growth inhibition

and ultimately on overall survival, in order to evaluate the appropriateness of the dose level proposed.

WHAT THIS STUDY ADDS TO OUR KNOWLEDGE

☑ This study characterizes the tumor dynamics in the squamous NSCLC population and the time course of tumor growth inhibition by necitumumab and chemotherapy backbone. Change in tumor size could be linked to hazard for overall survival.

HOW MIGHT THIS CHANGE DRUG DISCOVERY, DEVELOPMENT, AND/OR THERAPEUTICS?

☑ The model can be used for predicting survival outcome of alternate dosing strategies and protocols with necitumumab, and also enabling extrapolation of change in tumor size data to overall survival outcome in squamous NSCLC for other therapies.

Necitumumab (Portrazza) is a DNA-derived fully human monoclonal antibody (mAb) of the IgG1 subtype, with specificity to epidermal growth factor receptor (EGFR). It inhibits EGFR phosphorylation with high specificity, thereby neutralizing EGF-induced DiFi cell proliferation and inducing an antibody-dependent cell-mediated cytotoxic response against DiFi cells by human peripheral blood mononuclear cells. Preclinical experiments indicate that concentrations of ~0.9 nM block the interaction of EGF and EGFR to 50%, and that single agent treatment with necitumumab at doses of 4–6 mg/kg every second week, corresponding to trough serum levels of ~40 µg/mL, showed significant antitumor activity in non-small cell lung (NSCLC), pancreatic, colon, and squamous cervical cancer xenograft tumor models.^{1,2}

The pharmacokinetics of necitumumab has further been evaluated in a population pharmacokinetic (PK) analysis, across five studies in phases II and III.³ Necitumumab exhibits nonlinear PK, indicating target-mediated disposition

consistent with therapeutic mAbs.^{4–9} Covariate analysis did not indicate any patient factors such as gender, age, race, disease status, renal function, hepatic status, or baseline tumor load, while weight had a small contribution, all in concordance with previous findings of IgG-type mAbs in oncology.^{8,10} The interindividual variability in distribution and elimination was relatively high, leading to a wide distribution of steady-state serum levels observed in the phase III trials.^{11,12}

Known class effects of EGFR inhibitors are rash, hypomagnesemia, and thromboembolic events in particular.^{13–17} The tolerability of necitumumab in the clinic was assessed in solid tumor cancer patients, investigating doses of 100 mg up to 1,000 mg in a weekly or biweekly schedule,¹⁸ and the maximum tolerated dose (MTD) was defined as 800 mg. The major dose-limiting toxicity (WHO Grade 3+) observed was severe headaches. The most frequent treatment-related adverse events (AEs) were typical for this

¹PKPD&Pharmacometrics, Eli Lilly, Indianapolis, Indiana, USA; ²Eli Lilly Sweden, Solna, Sweden. *Correspondence: JE Wallin (wallinjo@lilly.com)
Received 19 January 2017; accepted 15 May 2017; published online on 13 July 2017. doi:10.1002/psp4.12209

class of agents, or events typically occurring in phase I settings, i.e., skin reactions, headache, nausea/vomiting, and fatigue. Pharmacokinetic simulations predicted that 800 mg given on day 1 and day 8 of a 3-week schedule would produce serum levels exceeding the preclinical threshold level in patients, where the schedule was selected to match the gemcitabine-cisplatin chemotherapy backbone administration schedule.

The clinical development of necitumumab followed the MTD approach still most often used in oncology, meaning that the highest tolerated dose level identified in a phase I setting was investigated in the phase III trials, without application of the efficacy-based dose evaluation commonly used in other therapeutic areas. The underlying principle stems from the chemotherapy era, where the more drug that is tolerated by the patient, the more efficacy you achieved, but needed to be balanced by safety. With targeted agents, however, it is possible that the exposure–response for safety and efficacy may be separated, and several examples have been presented by academia and regulators on the need for dose optimization on therapeutic proteins in the oncology area.^{19–22} This work aims at presenting the exposure–response modeling of safety and efficacy performed with data obtained in squamous NSCLC patients, given gemcitabine-cisplatin with or without necitumumab.¹²

METHODS

Study population

SQUIRE was a phase III global study comparing necitumumab in the combination with gemcitabine and cisplatin vs. gemcitabine and cisplatin alone, as a first-line treatment in patients with stage IV squamous NSCLC.¹² Necitumumab was given as an 800 mg infusion over 50 min on day 1 and day 8 of a 3-week cycle, with gemcitabine administered at 1,250 mg/m² on day 1 and day 8, and cisplatin at 75 mg/m² on day 1. Tumor size was assessed by radiographic imaging every 6 weeks until disease progression was observed according to RECIST criteria.²³ Necitumumab serum concentrations were assessed through predose sampling in every cycle, and average steady-state concentration ($C_{ss,ave}$) predictions were produced from the population PK model previously developed. The exposure–response analysis included safety, survival, and tumor size data from both the treatment arm and the control arm. Five patients who did not have any tumor size data were included in the final population model, which would therefore use typical values of tumor size metrics for these individuals. Data from patients in the treatment arm were included in the exposure–response analysis only if exposure measures were available.

Ethics

The data in this work were obtained in compliance with the Declaration of Helsinki, ICH GCP Guidelines, and applicable local regulations. Written informed consent was obtained from any patient entering the trial, and the local Ethics Committees associated with all participating center approved the protocol.

Statistical methods

Overall survival was described using a time-to-event modeling approach implemented using NONMEM v. 7.3 with the Stochastic Approximation Expectation-Maximization (SAEM) estimation algorithm. Models were executed using PsN. Various hazard models were tested including exponential, Weibull, Gompertz, combined Weibull and Gompertz, and log-logistic distributions of event times. The survival was calculated as the inverse of the exponent of the cumulative hazard from time = 0 to time = j in the study according to the following equation:

$$Surv_t = e^{-\int_0^t haz_t dt} \quad (1)$$

where $Surv_t$ was the survival at time t and $haz_t dt$ is the hazard at time t .

The likelihood of death at time t (probability density function, pdf) was calculated as follows:

$$pdf = haz_t \times Surv_t \quad (2)$$

Therefore, for individuals who died at time = t in the study had their pdf at that time estimated, while those who survived (or were censored) had their survival at time = t estimated.

Patient demographic covariates tested on the baseline hazard included:

- Geographical region that is, Region 1 (North America, Europe and Australia) vs. Region 2 (South America, South Africa, and India) vs. Region 3 (Eastern Asia). Other classifications were also tested including East Asian vs. non-East Asian; and Eastern Europe vs. Eastern Asian vs. the rest of the world;
- Race (Caucasian vs. non-Caucasian);
- Sex;
- Eastern Cooperative Oncology Group (ECOG) performance status at enrollment (0, 1, or 2);
- Smoking history (nonsmoker or light exsmoker vs. smoker);
- Histological subtype (basaloid, clear cell, small cell, papillary, or other);
- Age (continuous and using a cutpoint of 70 years).

As tumor size may be a significant predictor of survival, a model describing the change in tumor size (CTS) with time in the study was implemented and combined with the overall survival (OS) model. Throughout this article, tumor size in the model refers to the sum of the longest diameters of the target lesions. Target lesions were defined as all measurable lesions up to a maximum of five lesions per organ and 10 lesions in total, representative of all involved organs. Longitudinal tumor size was described as a summation of tumor growth and tumor shrinkage. Various growth models were tested including linear, exponential, and Gompertz growth, while a first-order process was used to describe tumor shrinkage. Differential equations describing these models are shown below:

$$\frac{dSize}{dt} = Size_0 \cdot e^{-shrink \cdot t} \cdot (-shrink) + growth; \quad (3)$$

linear growth and first-order shrinkage

$$\frac{dSize}{dt} = -shrink \times Size_t + growth \times Size_t; \quad (4)$$

exponential growth and first-order shrinkage

$$\frac{dSize}{dt} = -shrink \times Size_t + growth \times \log\left(\frac{Size_{max}}{Size_t}\right);$$

Gompertz growth and first-order shrinkage

(5)

where $Size_0$ is the baseline tumor size, $shrink$ is the first-order exponential decrease in the size of the tumor, $growth$ is the growth rate constant and $Size_{max}$ is the maximum possible tumor size.

The development of resistance was tested by means of a time-dependent reduction in the first-order process of tumor shrinkage as shown below:

$$Shrink_t = Shrink_0 \times e^{-resist \times t} \quad (6)$$

where $Shrink_t$ is the first-order shrink rate of the tumor at time, t , $Shrink_0$ is the shrink rate at the beginning of treatment, and $resist$ is the rate of decline of the shrink rate.

The tumor size at any time during treatment was then tested as a predictor of the hazard of death at the corresponding time in a model simultaneously describing OS and CTS. The estimation of tumor size and survival parameters was done simultaneously, which has the advantage of using all the available data at one time.

Parameters were mu-referenced and where inclusion of variability was not desired (for example, EC_{50}), a fixed value of 15% interindividual variability was used to optimize the efficiency of the SAEM search algorithm.²⁴ Since the minimum objective function (MOF) derived from SAEM is not suitable for hypothesis testing, the SAEM estimation process was followed by an evaluation step using importance sampling (IMP) to obtain an MOF that can be used for model comparison.²⁴ Due to the Monte Carlo noise in the MOF derived from expectation-maximization methods, values were interpreted with caution and changes in the MOF were viewed in the light of improvements in other model evaluation tools, including convergence, visual predictive checks (VPC), and goodness-of-fit plots (for tumor size data). The Monte Carlo noise in the IMP MOF was also kept to a minimum by increasing the number of random samples per subject (ISAMPLE) to 12,000, such that MOF would oscillate by an average of about 1–3 points between iterations in the IMP evaluation step. Fifteen iterations of the evaluation step were carried out for each model, and the MOF for a model would be calculated as the average MOF from iteration 10 to 15, whereupon it would have stabilized.

Individual patient post-hoc PK parameters were produced using a previously developed population PK model. Using the mean dose a patient received in the study (some patients had dose reductions initiated by the clinic investigator for various reasons) and the individual PK parameters,

an average steady-state concentration was obtained for each patient ($C_{ave,ss}$). For graphical exploration and presentation purposes, $C_{ave,ss}$ data were stratified in exposure quartiles for treatment arm, resulting in five strata: placebo (i.e., control arm), Q1, Q2, Q3, and Q4. Since the final model had a nonlinear component to it, the (quasi) $C_{ave,ss}$ was obtained by integrating the drug concentration between the 10th and 11th cycle of necitumumab administration then dividing by the time interval (504 h), and the distribution of predicted drug exposure is presented in **Supplemental Figure S1**. The drug concentration ($C_{ave,ss}$) was then tested in the integrated OS-CTS model using sigmoidal maximum effect models as shown below:

$$Drug\ effect = 1 \pm \frac{E_{max} \times Conc^{HILL}}{EC_{50}^{HILL} + Conc^{HILL}} \quad (7)$$

The drug effect was tested as a fractional decrease (–) in the baseline hazard for the OS and as a fractional increase (+) in the first-order shrink rate of the tumor (separate E_{max} and EC_{50} estimated). Difficulties were encountered in estimating the Hill coefficient; therefore, values fixed to 1 (ordinary E_{max} model), 2, 5, 10, and 15 were tested.

Covariates were tested using the hazard model (without tumor size), which enabled use of the Laplacian estimation method for reliable covariate testing (since the full model needed SAEM/IMP). Stepwise covariate model building (SCM) implemented using PsN was used for the covariate search. The forward inclusion criteria was $P < 0.05$ and the backward deletion criteria was $P > 0.01$. The selected covariates were then confirmed in the full model with the tumor size included.

A bootstrap analysis was performed to assess the precision of the final parameter estimates of base and final models. The bootstrap was carried out by sampling from the analysis dataset with replacement, to produce resampled datasets with the same number of patients. A total of 500 bootstrap datasets were created in this way, and each one fit to the final model. The 95% confidence intervals (CIs) for each parameter were calculated using the 2.5th and 97.5th percentile values from the distribution of bootstrap parameter values.

A VPC was performed for the integrated pharmacodynamics (PD) model for OS and CTS to ensure that the model could adequately predict the data used to develop it.

The VPC for the tumor size data entailed simulating the sum of longest diameters and overall survival using the developed simultaneous model, taking into account variability in model parameters as given by the interpatient variability, and residual error terms. In addition, since patients could die during the course of the study, it was necessary to incorporate dropout due to death in the tumor size simulations so that measurements would not be obtained from a dead patient. Furthermore, in accordance with the study protocol, patients who had documented disease progression as defined by a tumor size greater than 20% from their nadir would no longer have tumor size assessments, as they would have met the disease progression endpoint. Therefore, dropout due to disease progression was also incorporated in the simulations for tumor size data.

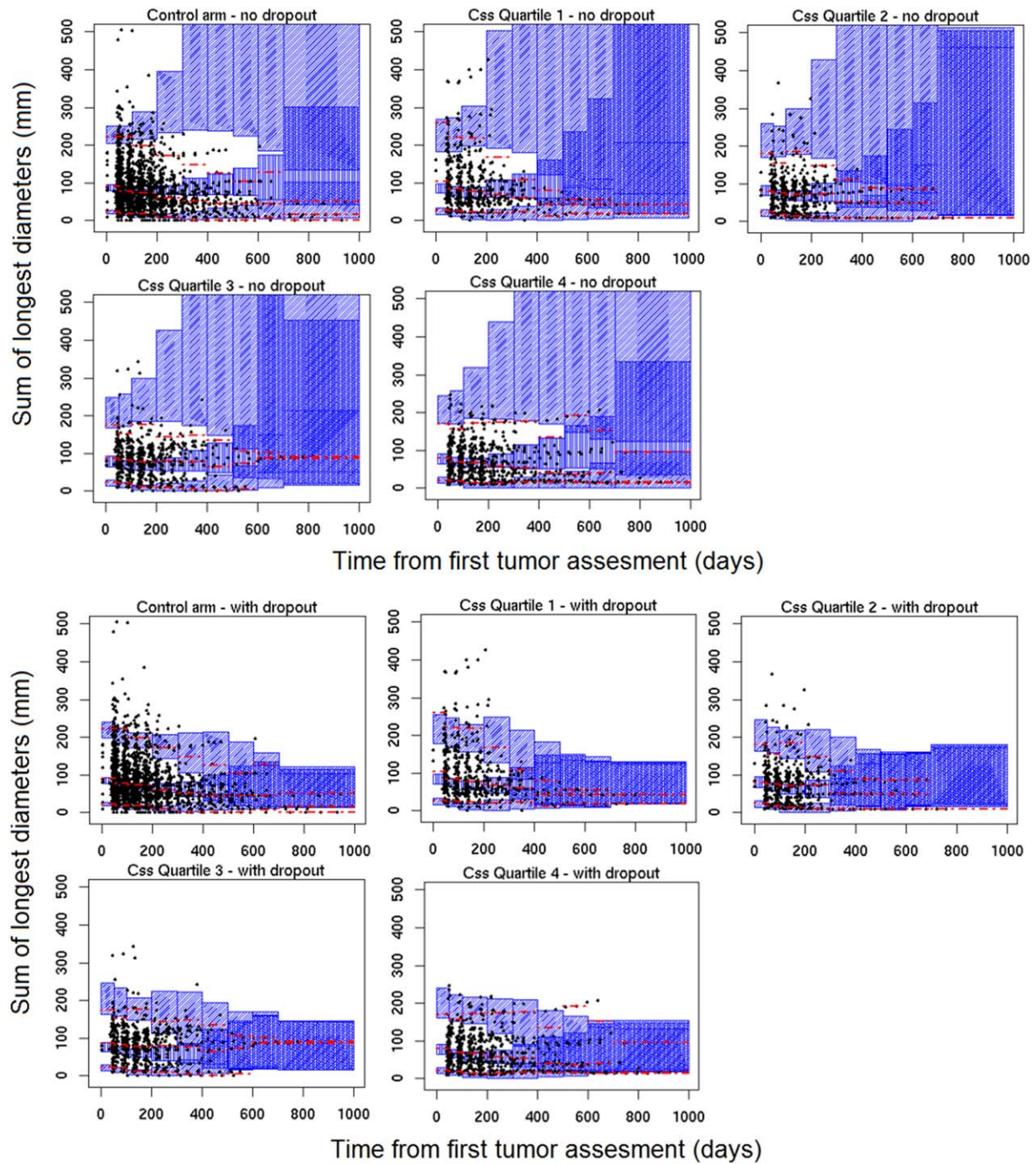


Figure 1 Visual predictive check for tumor growth inhibition model. Top panel no dropout model, bottom panel with dropout model.

Simulated and observed distributions were compared by calculating the median, 5th, and 95th percentiles for the observed data, then overlaying the 95% CI for the corresponding percentiles of the simulated data.

Similarly for OS, simulations were carried out using the final integrated model (meaning tumor size was also simulated) to obtain the simulated death times of patients. These were then used to construct a 95% prediction

interval of the Kaplan–Meier curve of the simulated data, which was then overlaid on the Kaplan–Meier curves of the observed data. The VPCs were stratified according to the quartiles of predicted necitumumab $C_{ave,ss}$.

The studied dose level for necitumumab is 800 mg, regardless of body weight. Using the final model, simulations of survival time using various values of necitumumab $C_{ss,ave}$ were carried out to investigate the adequacy of this dose.

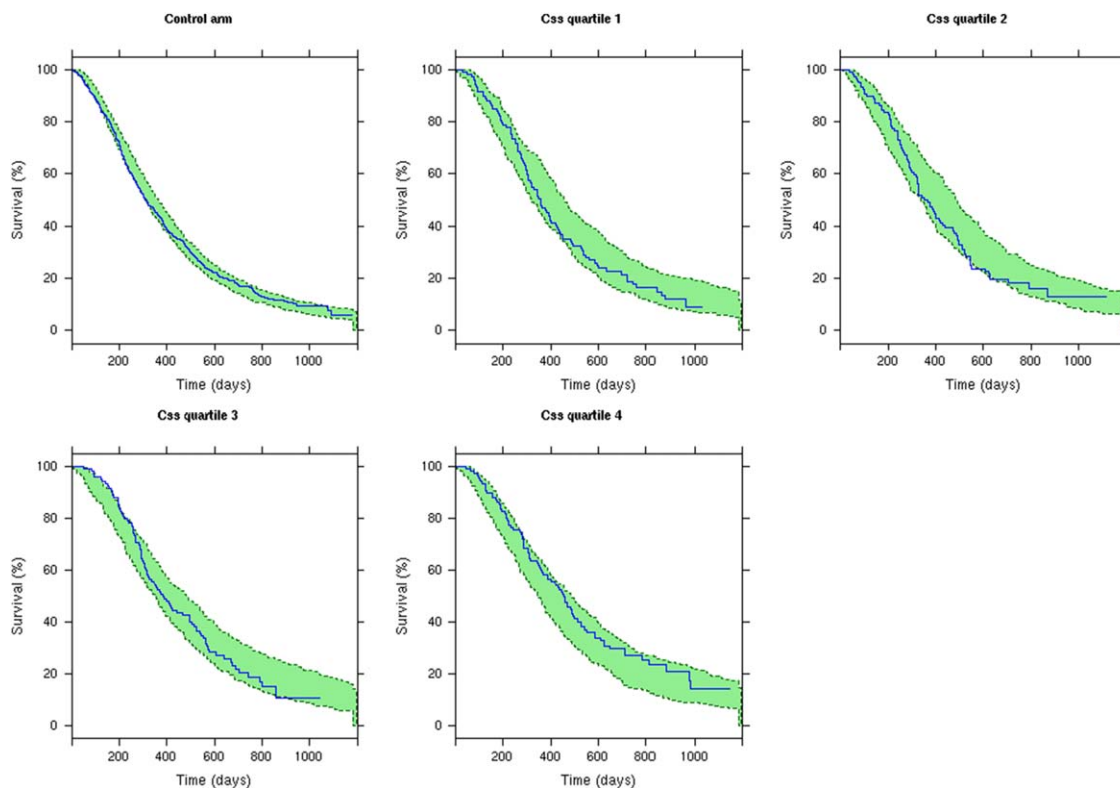


Figure 2 Visual predictive check for overall survival model.

Simulations were carried out to visualize the exposure–response relationship and the impact of alternative weight-based dosing paradigms.

RESULTS

The exposure–efficacy analysis included 1,014 patients, 538 of whom were randomized to the gemcitabine and cisplatin arm, while 476 were in the necitumumab plus gemcitabine and cisplatin arm.

The model that best described the change in tumor size was comprised of linear growth and first-order shrinkage.²⁵ This model had the lowest MOF and was stable. The model with the Gompertz growth was not stable, likely due to an inability to estimate the maximum possible tumor size. Inter-individual variability on the baseline tumor size, shrink rate, and growth rate was estimated in the model. A Box–Cox transformation of the random effects for the baseline tumor size was included, showing that the distribution was not exactly log-normal, but was negatively skewed. Furthermore, there was a positive correlation between the random effects for baseline tumor size and the growth rate. Development of resistance was also included, as described in the Methods section above. The onset of resistance was delayed and would start after a typical duration of about 6 weeks on treatment.

The time-to-event model that best described the overall survival was a combination of a Weibull function and Gompertz function for the hazard at time *t*. A significant predictor of the hazard at time *t* during the course of the study was the

tumor size at that time. Therefore, the hazard function in the final model was described according to the equation below:

$$\frac{d\text{Haz}}{dt} = \text{Basehaz} \times e^{[\text{Gomp} \times t + \text{Weib} \times \text{LOG}(t)]} \times e^{\text{DPHAZ} \times \text{Size}(t)} \quad (8)$$

where *Basehaz* is the baseline hazard at the beginning of the study, *Gomp* is the shape parameter representing the Gompertz distribution of event times, *Weib* is the shape parameter representing the Weibull distribution, and *DPHAZ* is the estimated link between model predicted tumor size at time *t* and the hazard.

Necitumumab *C_{ss,ave}* was a significant predictor of both the shrink rate of the tumor and the hazard for OS, as described earlier. The best Hill coefficient was a value of 10, implying a steep exposure–response relationship. **Table 2** shows the parameter estimates from the final model in addition to the precision determined from a bootstrap of 500 replicates. The parameter estimate for the variability of the time of onset of resistance is slightly outside the bootstrap 95% CI, probably because of the tight bootstrap confidence intervals combined with the stochastic noise of the SAEM Monte Carlo estimation method. The VPC for this model is shown in **Figure 1** (tumor size with and without dropout) and **Figure 2** (OS). The VPCs showed that the model adequately predicted the data.

A summary of the demographic data tested as covariates in the exposure–efficacy analyses and stratified by necitumumab *C_{ss,ave}* quartile are presented in **Table 1**. The majority of

Table 1 Summary of patient covariates included in efficacy analysis stratified per necitumumab concentration quartile

Covariate	Total	Control	Q1	Q2	Q3	Q4
Sex						
Male	847 (83.5%)	450 (44.4%)	113 (11.1%)	114 (11.2%)	96 (9.5%)	74 (7.3%)
Female	167 (16.5%)	88 (8.7%)	7 (0.7%)	5 (0.5%)	23 (2.3%)	44 (4.3%)
Race						
White	848 (83.6%)	449 (44.3%)	111 (10.9%)	100 (9.9%)	94 (9.3%)	94 (9.3%)
Non-white	166 (16.4%)	89 (8.8%)	9 (0.9%)	19 (1.9%)	25 (2.5%)	24 (2.4%)
Geographical origin 1						
N. America, Europe, Australia	883 (87.1%)	469 (46.3%)	114 (11.2%)	100 (9.9%)	99 (9.8%)	101 (10%)
S. America, S. Africa, India	97 (9.6%)	52 (5.1%)	5 (0.5%)	15 (1.5%)	14 (1.4%)	11 (1.1%)
Eastern Asia	34 (3.4%)	17 (1.7%)	1 (0.1%)	4 (0.4%)	6 (0.6%)	6 (0.6%)
Geographical origin 2						
Eastern Asia	77 (7.6%)	39 (3.8%)	3 (0.3%)	11 (1.1%)	11 (1.1%)	13 (1.3%)
Non Eastern Asia	937 (92.4%)	499 (49.2%)	117 (11.5%)	108 (10.7%)	108 (10.7%)	105 (10.4%)
Geographical origin 3						
Eastern Europe	513 (50.6%)	270 (26.6%)	79 (7.8%)	53 (5.2%)	59 (5.8%)	52 (5.1%)
Eastern Asia	77 (7.6%)	39 (3.8%)	3 (0.3%)	11 (1.1%)	11 (1.1%)	13 (1.3%)
Grand total	1014 (100%)	538 (53.1%)	120 (11.8%)	119 (11.7%)	119 (11.7%)	118 (11.6%)
Smoking status						
Nonsmoker or light exsmoker	90 (8.9%)	51 (5%)	6 (0.6%)	7 (0.7%)	14 (1.4%)	12 (1.2%)
Smoker	924 (91.1%)	487 (48%)	114 (11.2%)	112 (11%)	105 (10.4%)	106 (10.5%)
Histological subtype						
Missing	8 (0.8%)	5 (0.5%)	(0%)	2 (0.2%)	1 (0.1%)	(0%)
Basaloid	16 (1.6%)	7 (0.7%)	2 (0.2%)	1 (0.1%)	4 (0.4%)	2 (0.2%)
Clear cell	33 (3.3%)	19 (1.9%)	1 (0.1%)	3 (0.3%)	5 (0.5%)	5 (0.5%)
Small cell	24 (2.4%)	12 (1.2%)	3 (0.3%)	3 (0.3%)	4 (0.4%)	2 (0.2%)
Papillary	41 (4%)	19 (1.9%)	4 (0.4%)	6 (0.6%)	4 (0.4%)	8 (0.8%)
Other	892 (88%)	476 (46.9%)	110 (10.8%)	104 (10.3%)	101 (10%)	101 (10%)
Baseline ECOG status						
0	318 (31.4%)	176 (17.4%)	31 (3.1%)	32 (3.2%)	38 (3.7%)	41 (4%)
1	616 (60.7%)	316 (31.2%)	67 (6.6%)	82 (8.1%)	76 (7.5%)	75 (7.4%)
2	80 (7.9%)	46 (4.5%)	22 (2.2%)	5 (0.5%)	5 (0.5%)	2 (0.2%)

the patients were Caucasians (84%), male (84%), and were smokers (91%), although substantial numbers of other groups were present. There was no significant difference in the proportions of demographic covariates across the four necitumumab $C_{ss,ave}$ quartiles. ECOG status at baseline was the only significant clinical covariate. Patients with a higher ECOG status at baseline also had a greater tumor size at baseline. As can be seen from the confidence intervals in the table of parameter estimates (**Table 2**), this difference is mainly for patients with an ECOG score of 2, while there is no significant difference between patients with a score of zero or 1. Although the covariate did not meet the backward deletion criteria for retention in the model, it was kept in the model based on prior clinical knowledge.

A specific covariate of interest was the effect of age on survival. During the SCM model-building effort, this covariate was not found statistically significant, but **Figure S2** seems to suggest that patients in the necitumumab arm older than 70 years have less benefit. The continued misfit in the control arm suggests a paradoxical improvement in survival for older patients, which would not be expected. Therefore, the low numbers of patients in this age category precludes any definite conclusion.

The proposed dose for necitumumab is 800 mg, regardless of body weight. Using the final model, simulations of survival time using various values of necitumumab $C_{ss,ave}$ were carried out to investigate the adequacy of this dose. Simulations were carried out to visualize the exposure–response relationship, which is influenced by drug effect on both tumor size and overall survival. The composite exposure–response relationship is depicted in **Figure 3** and it shows that the vast majority of patients have adequate drug exposure. The figure shows that the population median predicted necitumumab $C_{ss,ave}$ of 216 $\mu\text{g/mL}$ results in an increase in survival time of about 60 days relative to control, with an effective EC_{50} of 82 $\mu\text{g/mL}$ and an E_{max} of 63 days. The model-predicted median survival time for patients in the control arm was 336 days (observed value 311 days). Patients in the 5th percentile would experience an increase in survival time of over 40 days, while those in the 95th percentile would have an increase of over 60 days. Based on the dosing regimen in SQUIRE, 474 (99.6%) of the 476 patients in the necitumumab arm had a $C_{ss,ave}$ greater than the EC_{50} . Therefore, near-maximum benefit is attained by nearly all patients receiving the proposed dosing regimen of 800 mg on day 1 and 8 of a 3-week cycle. However, the PK model^{3,26} revealed

Table 2 Pharmacodynamic and covariate parameters in final tumor growth inhibition and overall survival model

Parameter description	Population estimate (95% CI)	Interpatient variability (95% CI) %
Tumor size model		
Baseline tumor size (mm)	103 (96, 108)	61 (58, 64)
Box-Cox shape parameter for random effects of baseline tumor size ^a	-0.33 (-0.38, -0.19)	—
Tumor growth rate (mm/day)	0.049 (0.035, 0.068)	155 (137, 170)
Correlation between random effects of baseline tumor size and tumor growth rate		
Shrink rate of tumor (day ⁻¹)	0.0056 (0.0054, 0.0069)	73 (64, 82)
Time of onset of resistance (days)	43 (23, 44)	90 (96, 132)
Rate of development of resistance (day ⁻¹)	0.039 (0.026, 0.039)	—
Emax for necitumumab increasing shrink rate ^b	0.35 (0.16, 0.63)	—
EC50 (μg/mL) ^b	150 (143, 199)	—
Increase in baseline tumor size for ECOG = 1 relative to ECOG = 0 (%) ^c	7 (0, 16)	—
Increase in baseline tumor size for ECOG = 2 relative to ECOG = 0 (%) ^c	27 (9, 48)	—
Additive error (mm)	2.6 (0.9, 3.6)	—
Proportional error (%)	8.8 (7.8, 10)	—
Overall survival model		
Baseline hazard (day ⁻¹)	1.2 × 10 ⁻⁵ (5.0 × 10 ⁻⁶ , 3.2 × 10 ⁻⁵)	—
Effect of tumor size on hazard (mm ⁻¹)	0.0067 ^d (0.0053, 0.0080)	—
Weibull shape parameter	0.95 (0.74, 1.15)	—
Gompertz shape parameter	-0.0020 (-0.0028, -0.0013)	—
Emax for necitumumab decreasing baseline hazard ^e	0.19 (0.08, 0.3)	—
EC50 (μg/mL) ^e	71 (60, 75)	—

^a $ETA_{box} = \frac{(e^{ETA_i})^{-1}}{\theta_{box}}$ where ETA_{box} is the Box-Cox transformed random effect (from ETA_i) for baseline tumor size and θ_{box} is the estimated shape parameter.

^bFractional increase in shrink rate of tumor = $1 + \frac{Emax \times C_{ss}^\gamma}{EC50^\gamma + C_{ss}^\gamma}$ where γ was fixed to 10.

^cFractional increase in baseline tumor size = $1 + \theta_{ECOG}$ where θ_{ECOG} where θ_{ECOG} is the relevant value for a score of 1 or 2.

^dTranslates to a doubling in the hazard for every 103 mm of tumor

^eFractional decrease in hazard = $1 - \frac{Emax \times C_{ss}^\gamma}{EC50^\gamma + C_{ss}^\gamma}$ where γ was fixed to 10

an effect of body weight increasing clearance (hence lower exposure) and we sought to determine whether body weight or body surface area-based dosing would result in improved survival. First, the simulations using the PK model revealed that there would not be a significant reduction in variability, as shown in **Figure 4**. Second, and more important, the change in overall survival would not be significantly different regardless of dosing regimen (**Table S1**).

DISCUSSION

Exposure–efficacy response analysis demonstrated that an increase in exposure was associated with improvement in efficacy in terms of both tumor growth inhibition (TGI) and OS. The data on longitudinal tumor size following gemcitabine and cisplatin alone, or necitumumab plus gemcitabine and cisplatin treatment, were described using a TGI model.^{27–29} The positive correlation between the random effects of baseline tumor size and growth rate suggests that patients with larger tumors at baseline had an increased hazard of death. The decrease in the rate of tumor shrinkage rate after the first few weeks of treatment can be interpreted to represent the development of resistance.²⁸ High variability (90%) in the time to onset of resistance was estimated. This may be partly attributed to variability in the times of cessation of chemotherapy (cisplatin and/or gemcitabine). However, incorporating the end of chemotherapy in the

model did not reduce the MOF. Tumor size dynamics was found to be a strong predictor in the hazard function for death, with increasing tumor size being associated with a

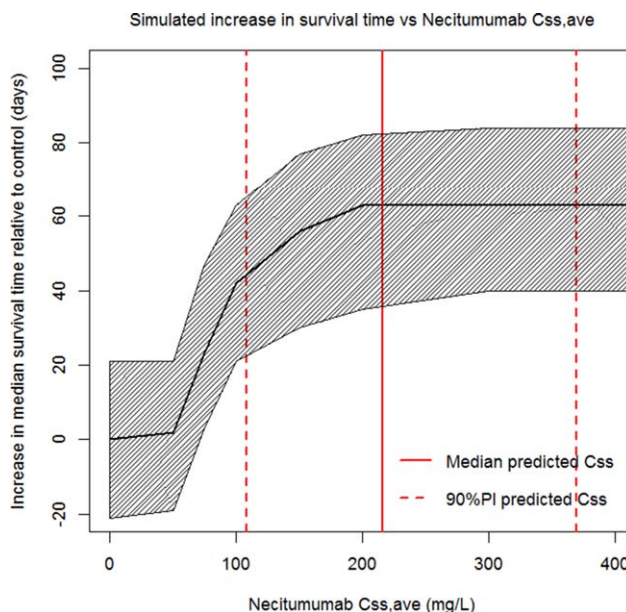


Figure 3 Necitumumab exposure–response curve for overall survival based on final model.

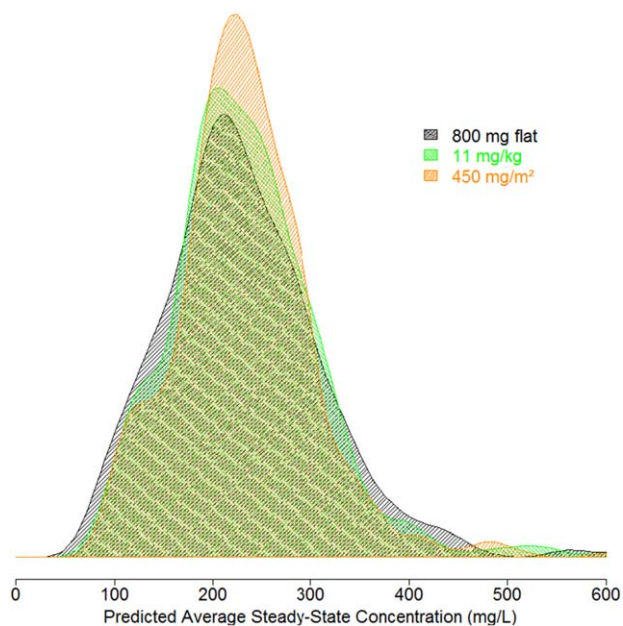


Figure 4 Density plot showing predicted $C_{ss,ave}$ necitumumab concentrations based on a flat 800 mg, weight-based (11.5 mg/kg), and body surface area-based (450 mg/m²) dose regimen administered on day 1 and day 8 of a 21-day cycle regimen.

greater hazard. Utilizing the complete time-course curve for tumor size was found superior to using single dimension metrics such as baseline tumor size, rate of tumor shrinkage, time to regrowth, or best percent change in tumor size. Historically, the majority of oncology PKPD modeling efforts of OS have been focusing on linking survival to a single dimension tumor size metric.^{30,31} It can be argued that looking at single dimension metrics ignores information, and may introduce bias as well as limit extrapolation of data.^{32,33} Utilizing a complete time-course should be more suitable at describing the complexity of interplay of tumor burden and OS, while still containing all single-dimension metrics. However, the ability to quantify this is often limited by availability of radiographical measurements. Benefits and limitations of this approach was investigated in depth in a simulation study by Ribba *et al.*,³⁴ and recent applications have demonstrated the feasibility in liver and renal cancer.^{35,36} This study demonstrates that application of simultaneous TGI-OS modeling can be done also within lung cancer, and be used for dose justification as well as evaluation of alternative dose regimens.

It should be noted that this work investigated the time-course only of target lesions, while it can be assumed that also nontarget lesions would contribute to hazard. As both drug concentration and tumor size were found to be significant predictors of hazard, it can be assumed that all drug effect on survival was not expressed through target lesions. Exposure–efficacy response for OS was assessed using a time-to-event model, with a combination of Weibull and Gompertz hazard distribution, and by including both predicted tumor size and the predicted necitumumab exposure as continuous variables in the model. The positive Weibull shape parameter indicates that the hazard was not constant, but increased with time in the study. However, the smaller but

negative Gompertz parameter indicates that there is also a timepoint beyond which the hazard starts to decrease.

A statistically significant positive exposure–efficacy relationship for TGI and OS was identified. A higher EC_{50} was estimated for tumor shrinkage than for OS. This may be expected, as it is likely that the tumor size measurement used, sum of longest tumor diameter (SLD) of five largest target lesions, does not necessarily reflect the complete tumor burden, and that nontarget lesions may differ from target lesions in growth dynamics and response to drug. It is also known that a tumor may become less metabolically active (therefore less harmful) without necessarily decreasing in size.³⁷ Furthermore, OS is correlated not only with tumor size in the dataset (target lesions), but also to other factors such as nontarget lesions, metastases, and general well-being, which are not related to the target lesion in the analyses. The improvement in model fit by adding a drug effect on the hazard separate from that via the tumor size shows that these other factors beyond the target lesion may be playing a role. Other studies have also reported a drug effect on baseline hazard for OS separate from the effect mediated through tumor size for a vascular endothelial growth factor (VEGF) inhibitor.³⁸

For computational reasons, $C_{ss,ave}$ was selected as the drug concentration metric input to the response model, rather than using $C(t)$. It should be noted that $C_{ss,ave}$ was predicted from the individual patient's mean dose level, and as 7.6% of patients had a dose reduction to 600 mg at some time during the trial. An integrated PKPD model with $C(t)$ as input for the TGI and OS model would possibly have been better suited to discern any additional concentration dependent covariates in the efficacy model, such as time to steady state.

Based on the reported effective EC_{50} , the model shows that the vast majority of patients had adequate exposure of necitumumab, and that 99.6% of treatment arm patients in SQUIRE had steady-state exposure superseding EC_{50} with a median exposure (216 μ g/mL) resulting in close to maximum effect. Since body weight was a significant covariate, it could be expected that heavier patients may have lower exposure. However, the predicted $C_{ss,ave}$ shows that most concentrations were well above EC_{50} in all patient weight strata, suggesting that 800 mg is an adequate dose regardless of weight. Simulations show that no significant decrease of variability in exposure would be achieved by weight-based dosing (**Figure 4**), and that observed survival in SQUIRE was not significantly related to body weight. Observed data indicate that heavy patients tend to have a slightly higher survival, in contrast to the expected lower drug exposure, and it can be speculated that heavier patients in a heavy disease burden Stage IV population might have a benefit to endure treatment or disease.

A limitation of the sequential PKPD modeling approach using C_{ss} may be that those patients who did not have any PK measurements were excluded from the study. While the reasons for absence of PK measurements are unknown (lost or spoilt laboratory samples, death), 60 patients (11% of those in the necitumumab arm) did not have measurements, hence could not be included in the analysis. While the data may not be missing at random, the relatively low percentage is not expected to have a significant influence on the results.

The very similar exposure distribution resulting from the explored dosing paradigms depicted in **Figure 4** translates also to small differences in overall survival (**Table S1**), where it is shown that even the lowest exposure quartile have a significant survival increase compared to control, regardless of flat or weight-based dosing. The analysis presented here thus validates the use of 800 mg necitumumab as a flat dose in the squamous NSCLC population.

Acknowledgment. This work was funded by Eli Lilly and Company.

Conflict of Interest. The authors are employees of Eli Lilly and Company.

Author Contributions. J.E.W. and E.C. wrote the article; J.E.W. designed the research; J.E.W., E.C., and A.J.L. performed the research; E.C. and A.J.L. analyzed the data.

- Dienstmann, R. & Felip, E. Necitumumab in the treatment of advanced non-small cell lung cancer: translation from preclinical to clinical development. *Expert Opin. Biol. Ther.* **11**, 1223–1231 (2011).
- Dienstmann, R. & Tabernero, J. Necitumumab, a fully human IgG1 mAb directed against the EGFR for the potential treatment of cancer. *Curr. Opin. Invest. Drugs* **11**, 1434–1441 (2010).
- Long, A., Chigutsa, E. & Wallin, J. Population pharmacokinetics of necitumumab in cancer patients. *Clin. Pharmacokinet.* (2016) [Epub ahead of print].
- Dostalek, M., Gardner, I., Gurbaxani, B.M., Rose, R.H. & Chetty, M. Pharmacokinetics, pharmacodynamics and physiologically-based pharmacokinetic modelling of monoclonal antibodies. *Clin. Pharmacokinet.* **52**, 83–124 (2013).
- Gibiansky, L. & Gibiansky, E. Target-mediated drug disposition model: approximations, identifiability of model parameters and applications to the population pharmacokinetic-pharmacodynamic modeling of biologics. *Expert Opin. Drug Metab. Toxicol.* **5**, 803–812 (2009).
- Gibiansky, L. & Gibiansky, E. Target-mediated drug disposition model and its approximations for antibody-drug conjugates. *J. Pharmacokinet. Pharmacodyn.* **41**, 35–47 (2014).
- Gibiansky, L., Gibiansky, E., Kakkar, T. & Ma, P. Approximations of the target-mediated drug disposition model and identifiability of model parameters. *J. Pharmacokinet. Pharmacodyn.* **35**, 573–591 (2008).
- Keizer, R.J., Huitema, A.D., Schellens, J.H. & Beijnen, J.H. Clinical pharmacokinetics of therapeutic monoclonal antibodies. *Clin. Pharmacokinet.* **49**, 493–507 (2010).
- Krippendorff BF, Kuester K, Kloft C, Huisinga W. Nonlinear pharmacokinetics of therapeutic proteins resulting from receptor mediated endocytosis. *J. Pharmacokinet. Pharmacodyn.* **36**, 239–260 (2009).
- Matsushima, S., Huang, Y., Suzuki, H., Nishino, J. & Lloyd, P. Ethnic sensitivity assessment — pharmacokinetic comparability between Japanese and non-Japanese healthy subjects on selected mAbs. *Expert Opin. Drug Metab. Toxicol.* **11**, 179–191 (2015).
- Paz-Ares, L. *et al.* Necitumumab plus pemetrexed and cisplatin as first-line therapy in patients with stage IV non-squamous non-small-cell lung cancer (INSPIRE): an open-label, randomised, controlled phase 3 study. *Lancet Oncol.* **16**, 328–337 (2015).
- Thatcher, N. *et al.* Necitumumab plus gemcitabine and cisplatin versus gemcitabine and cisplatin alone as first-line therapy in patients with stage IV squamous non-small-cell lung cancer (SQUIRE): an open-label, randomised, controlled phase 3 trial. *Lancet Oncol.* **16**, 763–774 (2015).
- Burotto, M., Ali, S.A. & O'Sullivan, CG. Class act: safety comparison of approved tyrosine kinase inhibitors for non-small-cell lung carcinoma. *Expert Opin. Drug Saf.* **14**, 97–110 (2015).
- Chanprapaph, K., Vachiramon, V. & Rattanakaemakorn, P. Epidermal growth factor receptor inhibitors: a review of cutaneous adverse events and management. *Dermatol. Res. Pract.* **2014**, 734249 (2014).
- Ma, W. *et al.* Safety profile of combined therapy inhibiting EGFR and VEGF pathways in patients with advanced non-small-cell lung cancer: A meta-analysis of 15 phase II/III randomized trials. *Int. J. Cancer* **137**, 409–419 (2015).
- Sandler, A.B. Nondermatologic adverse events associated with anti-EGFR therapy. *Oncology* **20**, 35–40 (2006).
- Vokes, E.E. & Chu, E. Anti-EGFR therapies: clinical experience in colorectal, lung, and head and neck cancers. *Oncology* **20**, 15–25 (2006).
- Kuonen, B. *et al.* A phase I pharmacologic study of necitumumab (IMC-11F8), a fully human IgG1 monoclonal antibody directed against EGFR in patients with advanced solid malignancies. *Clin. Cancer Res.* **16**, 1915–1923 (2010).
- Minasian, L. *et al.* Optimizing dosing of oncology drugs. *Clin. Pharmacol. Ther.* **96**, 572–579 (2014).
- Mould, D.R., Walz, A.C., Lave, T., Gibbs, J.P. & Frame, B. Developing exposure/response models for anticancer drug treatment: special considerations. *CPT Pharmacometrics Syst. Pharmacol.* **4**, e00016 (2015).
- Wang, J. *et al.* Exposure-response relationship of T-DM1: insight into dose optimization for patients with HER2-positive metastatic breast cancer. *Clin. Pharmacol. Ther.* **95**, 558–564 (2014).
- Venkatakrishnan, K. *et al.* Optimizing oncology therapeutics through quantitative translational and clinical pharmacology: challenges and opportunities. *Clin. Pharmacol. Ther.* **97**, 37–54 (2015).
- Therasse, P. *et al.* New guidelines to evaluate the response to treatment in solid tumors. European Organization for Research and Treatment of Cancer, National Cancer Institute of the United States, National Cancer Institute of Canada. *J. Natl. Cancer Inst.* **92**, 205–216 (2000).
- R B. NONMEM Users Guide. *Introduction to NONMEM 7.3*. ICON Deployment Solutions: Hanover, MD, 2013.
- Wang, Y., Dartois, C., Ramchandani, R., Booth, B.P., Rock, E. & Gobburu, J. Elucidation of relationship between tumor size and survival in non-small-cell lung cancer patients can aid early decision making in clinical drug development. *Clin. Pharmacol. Ther.* **86**, 167–174 (2009).
- Chigutsa, L.A., Heathman, M. & Wallin, J. The effect of body weight on necitumumab pharmacokinetics and pharmacodynamics in patients with squamous non-small cell lung cancer: dosing implications. *J. Pharmacokinet. Pharmacodyn.* **42**, S71 (2015).
- Bruno, R. & Claret, L. On the use of change in tumor size to predict survival in clinical oncology studies: toward a new paradigm to design and evaluate phase II studies. *Clin. Pharmacol. Ther.* **86**, 136–138 (2009).
- Claret, L. *et al.* Model-based prediction of phase III overall survival in colorectal cancer on the basis of phase II tumor dynamics. *J. Clin. Oncol.* **27**, 4103–4108 (2009).
- Tham, L.S. *et al.* A pharmacodynamic model for the time course of tumor shrinkage by gemcitabine + carboplatin in non-small cell lung cancer patients. *Clin. Cancer Res.* **14**, 4213–4218 (2008).
- Park, K. A review of modeling approaches to predict drug response in clinical oncology. *Yonsei Med. J.* **58**, 1–8 (2017).
- Bender, B.C., Schindler, E. & Friberg, L.E. Population pharmacokinetic-pharmacodynamic modelling in oncology: a tool for predicting clinical response. *Br. J. Clin. Pharmacol.* **79**, 56–71 (2015).
- Mansmann, U.R. & Laubender, R.P. Methodologic diligence is needed to define and validate tumor-size response metrics to predict overall survival in first-line metastatic colorectal cancer. *J. Clin. Oncol.* **31**, 4373–4374 (2013).
- Mistry, H.B. Time-dependent bias of tumor growth rate and time to tumor regrowth. *CPT Pharmacometrics Syst. Pharmacol.* **5**, 587 (2016).
- Ribba, B., Holford, N. & Mentre, F. The use of model-based tumor-size metrics to predict survival. *Clin. Pharmacol. Ther.* **96**, 133–135 (2014).
- Schindler, E., Amantea, M.A., Karlsson, M.O. & Friberg, L.E. A pharmacometric framework for axitinib exposure, efficacy and safety in metastatic renal cell carcinoma patients. *CPT Pharmacometrics Syst. Pharmacol.* (2017)
- Schindler, E. *et al.* Pharmacometric modeling of liver metastases' diameter, volume and density and their relation to clinical outcome in imatinib-treated GIST patients. *CPT Pharmacometrics Syst. Pharmacol.* (2017).
- Choi, H. *et al.* Correlation of computed tomography and positron emission tomography in patients with metastatic gastrointestinal stromal tumor treated at a single institution with imatinib mesylate: proposal of new computed tomography response criteria. *J. Clin. Oncol.* **25**, 1753–1759 (2007).
- Hansson, E.K. *et al.* PKPD modeling of predictors for adverse effects and overall survival in sunitinib-treated patients with GIST. *CPT Pharmacometrics Syst. Pharmacol.* **2**, e85 (2013).

© 2017 The Authors CPT: Pharmacometrics & Systems Pharmacology published by Wiley Periodicals, Inc. on behalf of American Society for Clinical Pharmacology and Therapeutics. This is an open access article under the terms of the Creative Commons Attribution-NonCommercial-NoDerivs License, which permits use and distribution in any medium, provided the original work is properly cited, the use is non-commercial and no modifications or adaptations are made.

Supplementary information accompanies this paper on the *CPT: Pharmacometrics & Systems Pharmacology* website (<http://psp-journal.com>)